Ion-Induced Rectification of Nanoparticle Quantized Capacitance Charging in Aqueous Solutions

Shaowei Chen* and Renjun Pei

Contribution from the Department of Chemistry, Southern Illinois University, Carbondale, Illinois 62901-4409

Received June 6, 2001

Abstract: Ion-induced rectification of nanoparticle quantized capacitance charging was studied using nanoparticle self-assembled monolayers in aqueous solutions in the presence of some unique electrolyte ions. The rectified charging features were interpreted on the basis of a Randles equivalent circuit where the binding of hydrophobic electrolyte ions to surface-confined particle molecules led to the manipulation of the electrode interfacial capacitance. It was found that the rectification effects were directly related to the ion hydrophobicity, manifested by the cathodic (anodic) shift of the onset potential with anions (cations) of increasing hydrophobicity Additionally, the voltammetric responses evolved from those similar to conventional molecular diodes to those of quantized charging rectifiers with increasing anion hydrophobicity. Electron-transfer kinetics evaluated by using various electrochemical methods yielded a rate constant within the range of 10−100 s^{-1} which decreased with increasing length of the alkyl spacers with a coupling coefficient (β) within the range of 0.8−0.9. Comparisons with conventional electroactive functional moieties were also discussed.

Introduction

The intense research interests in organized assemblies of nanosized particle molecules are primarily attributed to the great application potentialities of using these novel materials as the building blocks for next-generation optical/electronic devices.[1−3] For example, the molecular capacitor characters of monolayer-protected nanoclusters (MPCs)[4] demonstrate the unique electron-transfer chemistry of these jumbo molecules,[5] which might be of fundamental importance in the construction of electrical nanocircuits. Recently, we developed a two-step procedure involving surface place exchange reactions and self-assembling to fabricate robust long-range nanoparticle organized assemblies.[6,7] More importantly, we recently discovered that, for these MPC self-assembled monolayers on electrode surfaces, the MPC quantized capacitance charging could be rectified by certain hydrophobic anions (for instance, PF_6^-) in aqueous solutions, a response drastically different from that observed in low-dielectric organic media.[6] It was found that, in organic media, the voltammetric features of the MPC single-electron-transfer processes were observed at both negative and positive electrode potentials;[7] whereas in aqueous media, the features were visible only in positive potential regime. These unique rectification behaviors were interpreted on the basis of a Randles equivalent circuit where the electrode interfacial capacitance consisted of two components, one for the collective contribution of surface-immobilized MPC nanocapacitors and the other accounting for the interparticle void space (i.e., naked electrode surface). As the binding of electrolyte anions to MPC molecules was favored at positive electrode potentials where the particles were positively charged, the quantized charging characters were visible, due to the water expulsion properties associated with the (relatively) hydrophobic anions that altered the interfacial double-layer structure. This resulted in the onset of the MPC quantized electron transfers with a voltammetric current much greater than that at the same bare electrode. In contrast, in the negative potential region, binding of electrolyte anions to MPC molecules was not favored and the voltammetric currents measured were mainly ascribed to the classical electrode double-layer charging through the naked electrode surface and, hence, only suppressed and featureless responses. In essence, the voltammetric responses were very similar to those of a current rectifier regulated by electrode potentials where the hydrophobic electrolyte anions served as the chemical switch. This discovery might pave the way toward the development of single-electron molecular diodes.

Using the preliminary study as the point of departure, we carried out further and more systematic studies involving a wider variety of anions with varied degrees of hydrophobicity. In addition, we investigated the ion-binding chemistry of electrolyte cations, where one might suspect that the rectified electron-transfer behaviors in the negative potential regime might be initiated. Therefore, ideally, the combination of unique electrolyte cations and anions might serve as the chemical triggers for the regulation of these single-electron transistors at either negative or positive potentials. However, it turned out that the

* To whom all correspondence should be addressed. E-mail: schen@chem.siu.edu.

(1) (a) Schmid, G. *Clusters and Colloids: From Theory to Applications*; VCH: New York, 1994. (b) Turton, R. *The Quantum Dot: A Journey into the Future of Microelectronics*, Oxford University Press: New York, 1995.

(2) For instance: (a) Craighead, H. G. *Science* **2000**, *290*, 1532. (b) Quake, S. R.; Scherer, A. *Science* **2000**, *290*, 1536. (c) Jager, E. W. H.; Smela, E.; Inganäs, O. *Science* **2000**, *290*, 1540.

(3) See also the Special Reports in *Chem. Eng. News* **2000**, *78* (Oct 16), 25.

(4) (a) Brust, M.; Walker, M.; Bethell, D.; Schiffrin, D. J.; Kiely, R. *J. Chem. Soc., Chem. Commun*. **1994**, 801. (b) Whetten, R. L.; Shafigullin, M. N.; Khoury, J. T.; Schaaff, T. G.; Vezmar, I.; Alvarez, M. M.; Wilkinson, A. *Acc. Chem. Res*. **1999**, *32*, 397. (c) Templeton, A. C.; Wuelfing, W. P.; Murray, R. W. *Acc. Chem. Res.* **2000**, *33*, 27.

(5) (a) Ingram, R. S.; Hostetler, M. J.; Murray, R. W.; Schaaff, T. G.; Khoury, J.; Whetten, R. L.; Bigioni, T. P.; Guthrie, D. K.; First, P. N. *J. Am. Chem. Soc*. **1997**, *119*, 9279. (b) Chen, S.; Ingram, R. S.; Hostetler, M. J.; Pietron, J. J.; Murray, R. W.; Schaaff, T. G.; Khoury, J. T.; Alvrez, M. M.; Whetten, R. L. *Science* **1998**, *280*, 2098. (c) Chen, S.; Murray, R. W.; Feldberg, S. W. *J. Phys. Chem. B* **1998**, *102*, 9898.

(6) Chen, S. *J. Am. Chem. Soc*. **2000**, *122*, 7640.

(7) Chen, S. *J. Phys. Chem. B* **2000**, *104*, 663.

10.1021/ja011394c CCC: $20.00
Published on Web 10/04/2001

effects of electrolyte cations were far more complicated than those of the anions, presumably due to the discrepancy of their solvation structures. Additionally, effects of the electrolyte ions and solvent media on the electron-transfer kinetics of the MPC quantized capacitance charging were examined using various electrochemical methods, where the organic layer thicknesses of the MPC molecules were also varied. An exponential decay of the electron-transfer rate constants with the electron-transfer barriers was observed, akin to that of two-dimensional self-assembled monolayers with ω-functionalized moieties.[8] The results of these studies are detailed in this report.

Experimental Section

Chemicals. Ammonium hexafluorophosphate (NH_4PF_6, 99.5%, ACROS), potassium hexafluorophosphate (KPF_6, 99%, ACROS), ammonium perchlorate (NH_4ClO_4, 99.8%, ACROS), ammonium tetrafluoroborate (NH_4BF_4, 97%, ACROS), tetramethylammonium nitrate ($TAMNO_3$, ACROS), tetramethylammonium fluoride tetrahydrate (TMAF, 98%, ACROS), tetramethylammonium methyl sulfate ($TMACH_3SO_4$, ACROS), tetramethylammonium hydroxide pentahydrate (TMAOH, ACROS), tetraethylammonium nitrate ($TEANO_3$, 99%, ACROS), tetraethylammonium hexafluorophosphate ($TEAPF_6$, 99%, Aldrich), tetraethylammonium perchlorate (TEAP, Pfaltz & Bauzer), tetra-*n*-butylammonium perchlorate (TBAP, ACROS), tetra-*n*-butylammonium hydrogen sulfate ($TBAHSO_4$, Fluka), tetra-*n*-butylammonium dihydrogen phosphate ($TBAH_2PO_4$, ACROS), and 3-hydroxytyramine hydrochloride (99%, ACROS) were all used as received. Potassium nitrate (KNO_3, Fisher) and ammonium nitrate (NH_4NO_3, Fisher) were both recrystallized twice prior to use. All solvents were obtained from typical commercial sources and used as received as well. Water was supplied by a Barnstead Nanopure water system (18.3 MΩ).

Nanoparticles. The synthesis and structural manipulations of the monolayer-protected nanoparticles have been described previously.[4] Here, all *n*-alkanethiols (1-butanethiol, C4SH, 98%; 1-hexanethiol, C6SH, 98%; 1-octanethiol, C8SH, 97%; 1-decanethiol, C10SH, 96%) and α,ω-alkanedithiols (1,4-butanedithiol, C4(SH)2, 94%; 1,6-hexanedithiol, C6(SH)2, 97%; 1,8-octanedithiol, C8(SH)2, 99%; 1,9-nonanedithiol, C9(SH)2, 95%) were purchased from ACROS and used as received. Briefly, gold nanoparticles stabilized by a monolayer of alkanethiolates were synthesized by the Schiffrin route,[4a] which were denoted as C_nAu with C_n referring to the corresponding alkanethiolates. The particles were first fractionated by using a solvent and nonsolvent mixture (e.g., toluene and ethanol) to narrow the size dispersity with the final average particle core diameter of ~2.0 nm (determined by transmission electron microscopic measurements) and then underwent a thermal annealing process by refluxing in toluene for 8 h, resulting in mostly spherical shape and monodisperse size.[9] Further surface functionalizations were achieved by exchange reactions with a calculated feeding ratio of the particles and the new thiol ligands.[4c]

Nanoparticle Assemblies. The protocol for particles self-assembling onto a gold electrode surface has been described earlier (Scheme 1).[6,7] Briefly, alkanethiolate-protected nanoparticles obtained above were immobilized onto an electrode surface by a two-step procedure involving surface place exchange and self-assembling, where the particles were first exchanged with alkanedithiols of similar chain lengths, rendering the particle surface-active with various copies of free thiol groups at the outer peripheral surface, which then served as anchor sites for nanoparticle self-assembling, just like monomeric alkanethiols.

Electrochemical Studies. Electrochemical measurements were carried out with a BAS 100BW or CHI440 electrochemical workstation. A polycrystalline gold disk (sealed in a glass tubing) was used as the working electrode, and a Ag/AgCl (3 M NaCl, from BAS) and a Pt coil were used as the reference and counter electrodes, respectively. Prior to use, the gold electrode was first polished with 0.05-μm alumina slurries, followed by sonication in dilute nitric acid, sulfuric acid, and Nanopure water successively. The electrode was then subject to electrochemical etching by rapid potential sweep (10 V/s) in 0.10 M H_2SO_4 within the potential range of +1.2 and −0.2 V for 5 min. In aqueous solutions containing varied electrolytes, the reference electrode was calibrated with the redox potential of $K_3Fe(CN)_6/K_4Fe(CN)_6$. In organic solutions, a quasi-reference Ag/AgCl wire was used instead. The electrolyte solutions were prepared in water or in methylene chloride, depending upon the specific electrolytes. The solutions were deaerated for at least 20 min prior to data acquisition by high-purity argon, which was saturated by either water or methylene chloride and blanketed with an atmosphere of Ar during the entire experimental procedure.

Scheme 1. Schematic Illustrations for the Self-Assembling of Nanoparticles onto Electrode Surfaces[6,7]

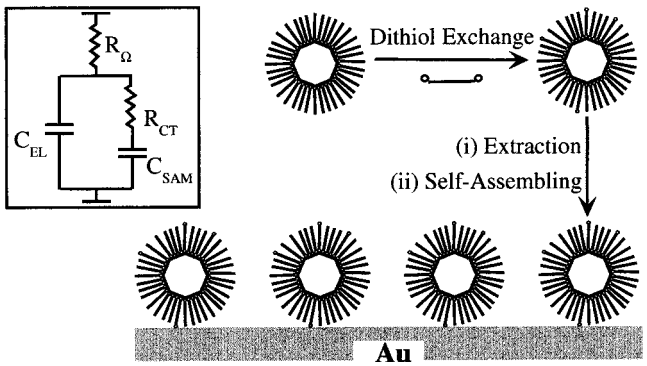

Results and Discussion

In this section, we first describe the rectified quantized charging of MPC self-assembled monolayers in aqueous solutions, in comparison with the responses in organic media. We then present studies of the effects of electrolyte ions on these single-electron-transfer processes, followed by an investigation of the electron-transfer kinetics using various electrochemical methods.

Rectified Quantized Charging. As described previously,[6] MPC self-assembled monolayers exhibit rectified quantized charging features in aqueous solutions induced by hydrophobic electrolyte ions. Figure 1B shows a series of representative cyclic voltammograms of a C6Au MPC self-assembled monolayer (linked with C6(SH)2) on a gold electrode surface in 0.10 M NH_4PF_6. There are several unique characters that warrant attention. First, the quantized charging features are observed only at positive electrode potentials (relative to MPC potential of zero charge, PZC), in contrast to those observed in organic media (e.g., CH_2Cl_2)[7] where the discrete electron-transfer processes were rather well-defined in both the positive and negative potential regimes. Second, the voltammetric current at the positive potential regime is much greater than that at the same bare electrode whereas in the negative potential regime the current is even somewhat suppressed.[6] In essence, the behaviors are similar to a current rectifier where the on and off appear to be controlled by the electrolyte anions (PF_6^-) and regulated by electrode potentials. The rectification mechanism is interpreted based on the Randles equivalent circuit (Scheme 1 inset) where the binding of electrolyte anions (PF_6^-) to the MPC molecules is manipulated by the electrode potentials and leads to the variation of the two constituents of the electrode interfacial double-layer capacitance (Scheme 1 inset),[6] i.e., C_{SAM} and C_{EL}, which account for the collective contributions of all

(8) (a) Holmlin, R. E.; Haag, R.; Chabinyc, M. L.; Ismagilov, R. F.; Cohen, A. E.; Terfort, A.; Rampi, M. A.; Whitesides, G. M. *J. Am. Chem. Soc.* **2001**, *123*, 5075. (b) Slowinski, K.; Chamberlain, R. V.; Miller, C. J.; Majda, M. *J. Am. Chem. Soc.* **1997**, *119*, 11910. (c) Smalley, J. F.; Feldberg, S. W.; Chidsey, C. E. D.; Linford, M. R.; Newton, M. D.; Liu, Y. *J. Phys. Chem.* **1995**, *99*, 13141. (d) Weber, K.; Hockett, L.; Creager, S. E. *J. Phys. Chem. B* **1997**, *101*, 8286.

(9) (a) Chen, S. *Langmuir* **2001**, *17*, 2878. (b) Maye, M. M.; Zheng, W.; Leibowitz, F. L.; Ly, N. K.; Zhong, C.-J. *Langmuir* **2000**, *16*, 490.

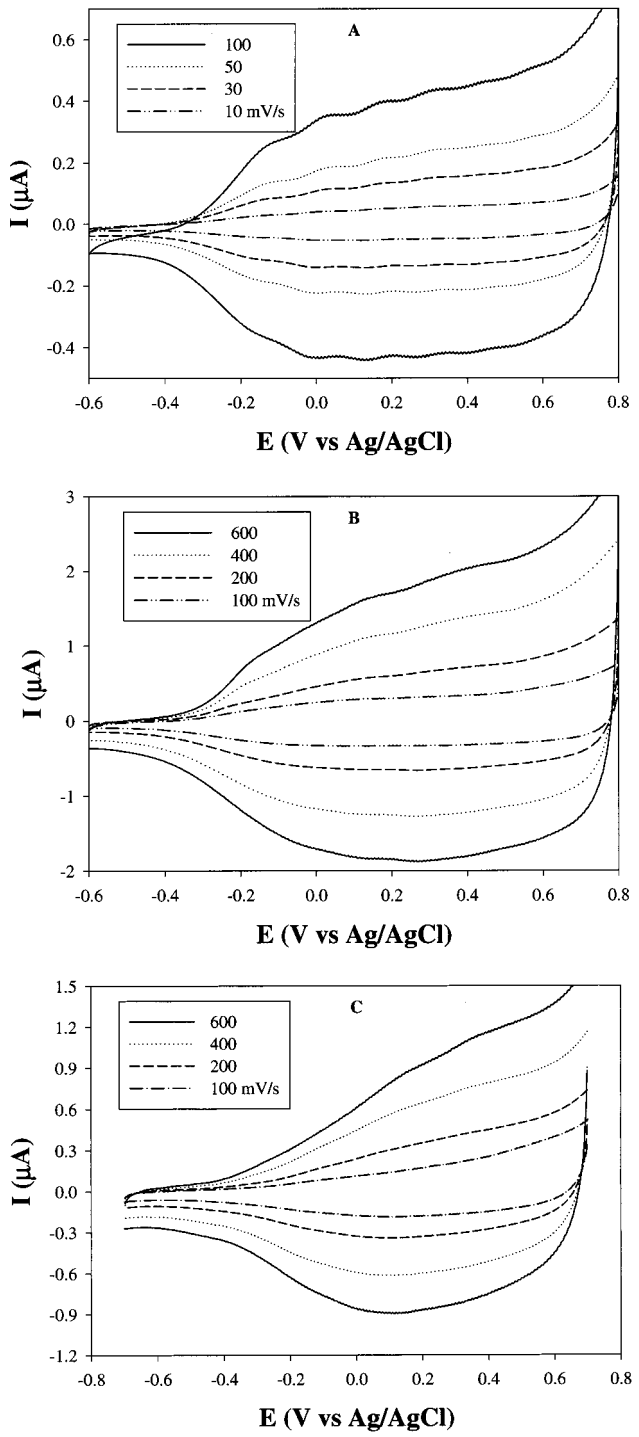

Figure 1. Cyclic voltammograms (CVs) of self-assembled monolayers of gold MPCs with varied protecting alkanethiolate monolayers in 0.10 M NH_4PF_6 (anchored by the corresponding dithiols of similar chain lengths): (A) C4Au; (B) C6Au; (C) C8Au. Electrode area 1.1 mm^2. Sweep rates as shown.

surface-immobilized MPC molecules and the electrode surface defects (i.e., interparticle voids), respectively. At positive potentials, the surface-immobilized MPCs are positively charged, where ion binding with electrolyte anions (PF_6^-) is favored. As the hydrophobic PF_6^- ions expel water molecules from the interfacial region, the voltammetric currents measured are mainly due to the charging through surface-anchored MPC molecules (C_{SAM}) and hence the quantized charging features; whereas in the negative potential regime, ion binding is disfavored and therefore the interfacial charging is mainly through the naked electrode surface (C_{EL}), manifested by featureless classical double-layer charging. In essence, the hydrophobic PF_6^- ions serve as chemical switches for these MPC current rectifiers.

Table 1. Molecular Capacitance of MPCs with Varied Protecting Alkanethiolate monolayers[a]

C_{MPC} (aF)	C4Au	C6Au	C8Au
solutions[b]	0.64	0.58	0.53
monolayers (organic)[c]	0.80	0.71	0.66
monolayers (H_2O, NH_4PF_6)[d]	1.10	1.03	0.82
monolayers (H_2O, KPF_6)[d]	1.09	1.07	
monolayers (H_2O, $TEAPF_6$)[d]	1.16	1.06	
monolayers (H_2O, $TEAClO_4$)[d]	1.15		
monolayers (H_2O, NH_4ClO_4)[d]		0.90	
monolayers (H_2O, NH_4BF_4)[d]		0.85	
monolayers (H_2O, $TMABF_4$)[d]		1.09	

[a]Determined by the peak spacings from the respective differential pulse voltammograms. [b]MPCs were dissolved in CH_2Cl_2 containing 0.10 M TBAP at a concentration of ~0.10 mM. [c]MPC monolayers on a gold electrode in CH_2Cl_2 containing 0.10 M TBAP. [d]MPC monolayers on a gold electrode in H_2O with 0.10 M electrolytes.

Similar observations were found with other MPC molecules. Panels A and C of Figure 1 show the corresponding cyclic voltammograms for C4Au and C8Au MPCs monolayers bridged by C4(SH)2 and C8(SH)2, respectively, onto a gold electrode surface. As the voltammetric peaks reflect the successive single-electron-transfer reactions of the surface-immobilized MPC molecules, the MPC molecular capacitance can be evaluated, $C_{MPC} = e/\Delta V$, where e is electronic charge and ΔV is the potential spacing between neighboring peaks. Table 1 compiles the effective molecular capacitance of the MPCs with varied alkanethiolate monolayers when the particles are dissolved in (organic) solutions, as well as immobilized on an electrode surface and measured in organic or aqueous solutions. One can see that, first, the molecular capacitance decreases with increasing chain length of the MPC protecting monolayers in either organic or aqueous media, as observed previously.[5] Second, there is a ~25% increase in MPC capacitance when the particles are anchored onto the electrode surface as compared to that when the particles are dissolved in solutions. This might suggest that, if one assumes a similar (effective) dielectric constant for the MPC protecting monolayers in both cases, the overall particle size in the surface assemblies is somewhat larger than that of the original sample. In other words, larger sized particles might be more likely to anchor onto the electrode surface during the self-assembling process. More interestingly, the molecular capacitance evaluated from the same MPC monolayers is even larger (25−50%) in aqueous media than in organic solutions. This might be ascribed to the binding of electrolyte ions to the surface-confined MPC molecules in aqueous solutions, akin to the case where ω-ferrocenated MPCs exhibited a severalfold increase of molecular capacitance when the ferrocene moieties were oxidized to ferrocenium.[10] In addition, there appear some subtle variations in MPC capacitance in aqueous solutions containing different electrolyte ions (the effects of electrolyte compositions will be discussed in detail in the next section). For instance, the capacitance measured in PF_6^--containing solutions (such as KPF_6, NH_4PF_6, and $TEAPF_6$) seems to be slightly greater than that in solutions containing ClO_4^- (e.g., NH_4ClO_4), which is then somewhat greater than that in BF_4^--containing solutions (e.g., NH_4BF_4). This might be understood in terms of their decreasing hydrophobicity (and increasing solubility in water) and hence ion-binding strength. One might

(10) (a) Hostetler, M. J.; Green, S. J.; Stokes, J. J.; Murray, R. W. *J. Am. Chem. Soc.* **1998**, *118*, 4212. (b) Green, S. J.; Stokes, J. J.; Hostetler, M. J.; Pietron, J. J.; Murray, R. W. *J. Phys. Chem. B* **1997**, *101*, 2663.

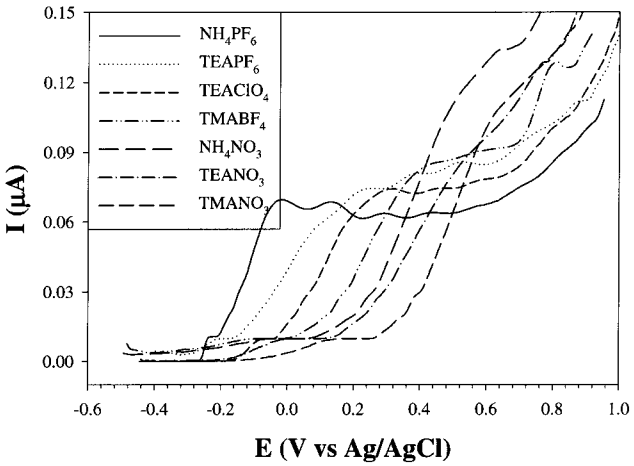

Figure 2. DPVs of the same C4Au MPC monolayers (as in Figure 1) in varied electrolyte solutions (0.10 M). Dc potential ramp 10 mV/s, pulse amplitude 50 mV, and pulse width 50 ms. Potential has been corrected by using the formal potential of $K_3Fe(CN)_6/K_4Fe(CN)_6$ as the calibration reference.

also note that the presence of TMA^+ or TEA^+ ions leads to a small increase of the MPC capacitance as well (in the presence of identical anions), which might be ascribed to the solvation effect of these bulky countercations when they interact with the MPC-bound anions leading to the formation of a more complicated solvation shell structure (vide infra). These experimental observations appear to be consistent with the ion-induced mechanism for the rectification of MPC quantized charging.

Ion−MPC Binding. The ion-induced rectification of MPC quantized charging is not limited to PF_6^-; other bulky and hydrophobic anions have similar effects as well. Figure 2 shows some representative differential pulse voltammograms (DPVs) of the same MPC monolayers as in Figure 1 in varied electrolyte solutions. From Figure 2, one can see that the rectified discrete electron transfers are rather well-defined in the presence of PF_6^-, ClO_4^-, and BF_4^- with the cations varied from K^+ to NH_4^+, TMA^+, and TEA^+, for instance; whereas in the presence of "hard" anions such as NO_3^-, HSO_4^-, $H_2PO_4^-$, etc., only featureless response is found regardless of the cations. In the latter solutions, the voltammetric responses are similar to a Coulomb blockade, where at a potential more negative than the onset potential (defined as the potential at which the charging current profiles starts to rise), the current is suppressed greatly, and at more positive potentials, the current increases drastically. These behaviors might be attributed to the leakage current of double-layer charging through the defects of the MPC self-assembled monolayers, as observed previously in self-assembled monolayers of alkanethiols on noble metal surfaces.[12] Another plausible explanation is that both the particle capacitance and electrode double-layer capacitance are potential dependent and increase drastically at extreme potentials, resulting in the enhanced double-layer charging currents at extreme electrode potentials. Thus, one can see that an increase of anion hydrophobicity results in a transition of the MPC charging responses from those similar to conventional molecular diodes to those of quantized charging rectifiers.

Overall, one might note that the rectification of quantized charging features appears to be more sensitive to anions than to cations. For instance, the presence of bulky tetra-*n*-alkylammonium cations (e.g., TEA^+, and TMA^+) fails to initiate the rectification responses in the *negative* potential regime, and the discrete charging features in the positive potential region are quite ill-defined. This might be accounted for by the more complicated solvation structures of cations in aqueous solutions. For instance, the greater polarizability (and consequential hydrophobicity) of bulky anions relative to cations results in their stronger interactions with surface-bound MPC molecules (vide ante). This is again in consistence with the ion-binding mechanism of the rectification of MPC quantized charging. Further studies with other bulky cations are desired to provide deeper insight into the molecular origin of the unique chemistry involved.

As mentioned above,[6] the ion-induced rectification mechanism is further evidenced by the exponential (cathodic) shift of the MPC voltammetric profiles with increasing electrolyte anion concentration,[13]

$$E_f = E^{o\prime} + \left(\frac{RT}{n_a F}\right)\ln\left(\frac{K_2}{K_1}\right) - (p-q)\frac{RT}{n_a F}\ln[\text{anion}] \quad (1)$$

where E_f and $E^{o\prime}$ are the formal potentials in the presence and absence of ion binding, respectively; n_a is the (effective) number of electron transfer; K_1 and q (K_2 and p) are the equilibrium constant and the number of anions bound to the reduced (oxidized) forms of the MPC molecules, respectively; and other parameters have their usual significance. Figure 3 shows some representative DPVs of a C6Au MPC monolayer in a mixed aqueous solution of NH_4NO_3 and another electrolyte containing "soft" ions (with the overall solution ionic strength maintained at 0.10 M). One can see that, with increasing concentration of PF_6^-, the voltammetric current profiles shift cathodically (Figure 3A), as anticipated from eq 1. The linear regressions of E_f versus $\ln[PF_6^-]$ yield slope values of −28, −35, and −41 mV for the first, second, and third charging peaks (Figure 3B), respectively, which are somewhat larger than the value of −25 mV expected for a 1:1 ratio of the number of MPC-bound PF_6^- ions and MPC charge state (at 25 °C and $n_a = 1$). The deviation becomes more significant with MPCs of higher charge states, suggesting that the intrinsic charge of MPC molecules facilitates stronger interactions with PF_6^- ions.

Similar behaviors was also observed in the variation of MPC formal potentials with other "soft" electrolyte anions, such as ClO_4^- and BF_4^- (not shown). However, in the presence of bulky cations, the responses appear to be more complicated. Figure 3E shows the DPVs of the same C6Au MPC monolayers in a mixed solution containing varied compositions of $TEANO_3$ and NH_4NO_3. One can see that in this case the voltammetric profiles shift *anodically* with increasing concentration of TEA^+, and the linear regression of the voltammetric peak potential with TEA^+ concentration yields a slope of about +56 mV (Figure 3F). This is, again, much larger than that expected for a 1:1 binding stoichiometry. These observations strongly suggest that binding of bulky electrolyte cations to surface-confined MPCs did occur; however, the binding chemistry appears to be more complicated than that involving anionic counterparts (vide ante), which is quite surprising and counterintuitive considering the repulsive electrostatic interactions between the particles and the cations at positive electrode potentials. Part of the reason might be ascribed to the charge screening effect of the counteranions (NO_3^-) in the electrolyte solutions (more details below).

(11) Bard, A. J.; Faulkner, L. R. *Electrochemical Methods*, 2nd ed.; John Wiley & Sons: New York, 2001.

(12) Widrig, C. A.; Chung, C.; Porter, M. D. *J. Electroanal. Chem.* **1991**, *310*, 335.

(13) (a) Sagara, T.; Maeda, H.; Yuan, Y.; Nakashima, N. *Langmuir* **1999**, *15*, 3824. (b) Hiley, S. L.; Buttry, D. A. *Colloid Surf. A: Physicochem. Eng. Aspects* **1994**, *84*, 129.

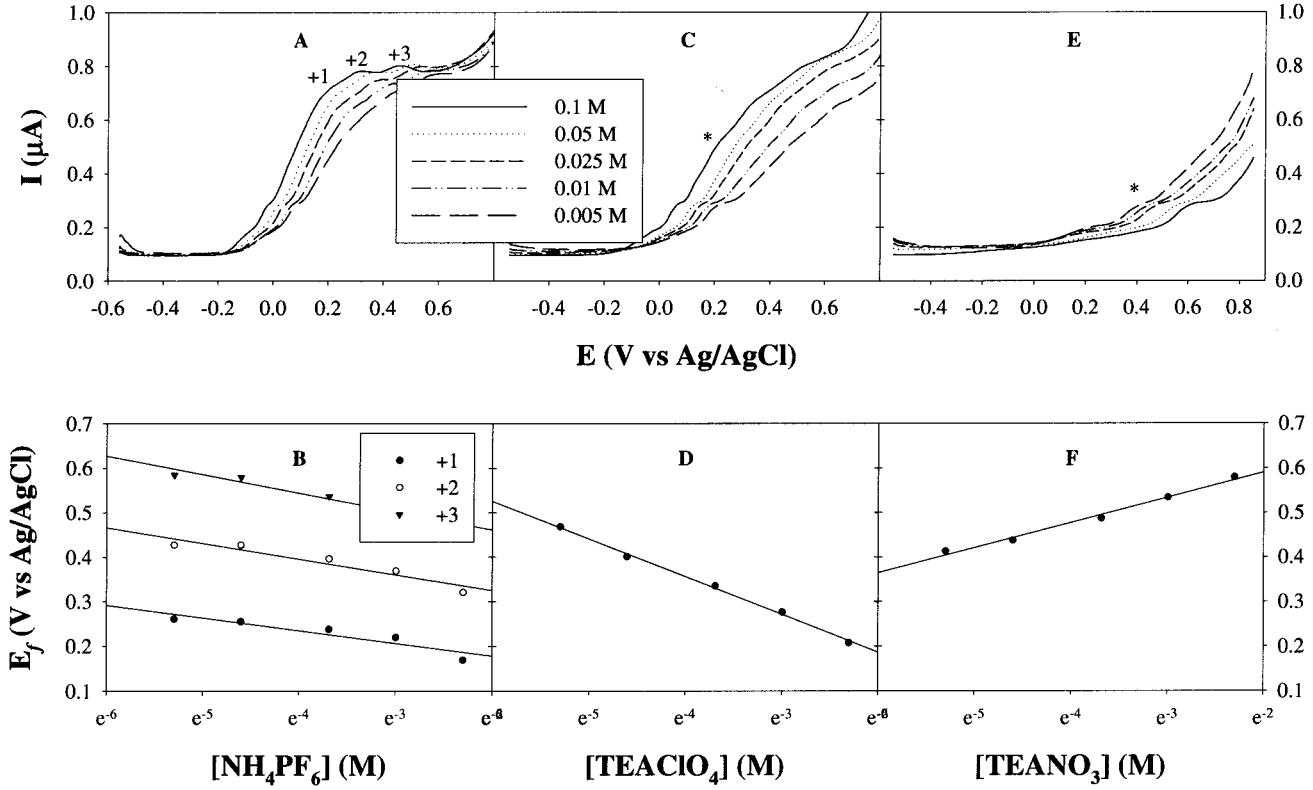

Figure 3. Variation of the voltammetric profiles (DPVs) of a C6Au MPC monolayer in various electrolyte compositions: (A) x M NH_4PF_6 + (0.10 − x) M NH_4NO_3; (C) x M $TEAClO_4$ + (0.10 − x) M NH_4NO_3; (E) x M $TEANO_3$ + (0.10 − x) M NH_4NO_3 with x shown in the figure legend. (B), (D), and (F) show the corresponding variations of voltammetric peak potentials with hydrophobic ion concentrations, where symbols are experimental data and lines are the respective linear regressions. In (B), the legends refer to the discrete charging peaks shown in (A); while data in (D) and (F) refer to the peaks in (C) and (E) indicated by an asterisk, respectively.

In the presence of both "soft" cations and anions, the behaviors are even more intriguing. For instance, in a solution containing TEA^+ and ClO_4^- (again with NH_4NO_3 to maintain the solution ionic strength, Figure 3C and D), the voltammetric responses do not appear to be the additive results of the cations and anions. From Figure 3C, one can see that the current profiles actually shift *cathodically* with increasing [TEA^+] and [ClO_4^-], and the linear regression of E_f versus ln[$TEAClO_4$] (Figure 3D) yields a slope of −85 mV, indicating that the presence of TEA^+ actually facilitates an even stronger binding of ClO_4^- anions to MPC molecules. This might be ascribed to the preferential binding of hydrophobic anions to MPC molecules whose relatively strong interactions with "soft" electrolyte cations lead to the formation of more complicated (e.g., layered) solvation structures around the MPC molecules and, hence, the more effective binding of anions to the particles.

These observations indicate that most probably both hydrophobic interactions and electrostatic forces play a rather significant role in the ion-binding process. In anion-binding processes, both the electrostatic and hydrophobic interactions between the anions and the MPC molecules make constructive contributions to the formation of anion−MPC pairs at positive electrode potentials. In contrast, in the case of cations, the electrostatic interactions and hydrophobic interactions play an opposite role in the manipulation of cation−MPC pairs. The resulting MPC charging currents are then the collective contributions of these various interactions which manipulate the interfacial double-layer structures.

Potential Control of Rectification. As stipulated above,[6] the onset of the rectified quantized charging is ascribed to the binding of electrolyte anions to positively charged MPC molecules at positive electrode potentials. This is anticipated to be closely related to the MPC potential of zero charge (E_{PZC}) in the specific electrolyte solutions, akin to the effect of specific adsorption on the electrode interfacial double-layer structures.[11] From Figure 2, one can see that the onset of the charging current for these current rectifiers varies with different ions in the solutions, where the onset potential (E_{on}, which is close to E_{PZC}) shows a negative shift with more hydrophobic anions, for instance, from NO_3^- to PF_6^-. This might be accounted for by the binding of "soft" anions to the electrode interface, which shifts the E_{PZC} to a more negative potential position and hence the negative onset of the quantized electron-transfer reactions of the particles. Table 2 lists the onset potentials for the MPC monolayers in a series of aqueous electrolyte solutions, where one can see that the anion effects can be grouped into the following sequence: (NH_4PF_6, NH_4PF_6, $TEAPF_6$) < (NH_4ClO_4,

Table 2. Variation of Onset Potentials (E_{on}) of MPC Rectification in Varied Electrolyte Solutions[a]

E_{on} (V)	C4Au	C6Au	C8Au	C10Au
NH_4PF_6	−0.26	−0.20	−0.28	−0.32
KPF_6	−0.26	−0.20	−0.28	−0.32
$TEAPF_6$	−0.18	−0.16	−0.20	−0.28
NH_4ClO_4	−0.12	−0.07	−0.16	−0.24
NH_4BF_4	−0.08	0	−0.14	−0.18
TEAP	−0.10	−0.05	−0.15	−0.20
$TMABF_4$	−0.02	0.01	−0.12	−0.16
NH_4NO_3	0.06	0.14	0	0
KNO_3	0.12	0.16	0.12	0.08
$TEANO_3$	0.15	0.28	0.16	0.20
$TMANO_3$	0.26	0.30	0.24	0.22

[a](i) All electrolyte concentrations are 0.10 M. (ii) For C6Au particles, the onset potentials in additional electrolyte solutions are as follows: TMAF, 0.28 V; TMAOH, 0.33 V; $TMACH_3SO_4$, 0.27 V; $TBAH_2PO_4$, 0.35 V; and $TBAHSO_4$, 0.35 V.

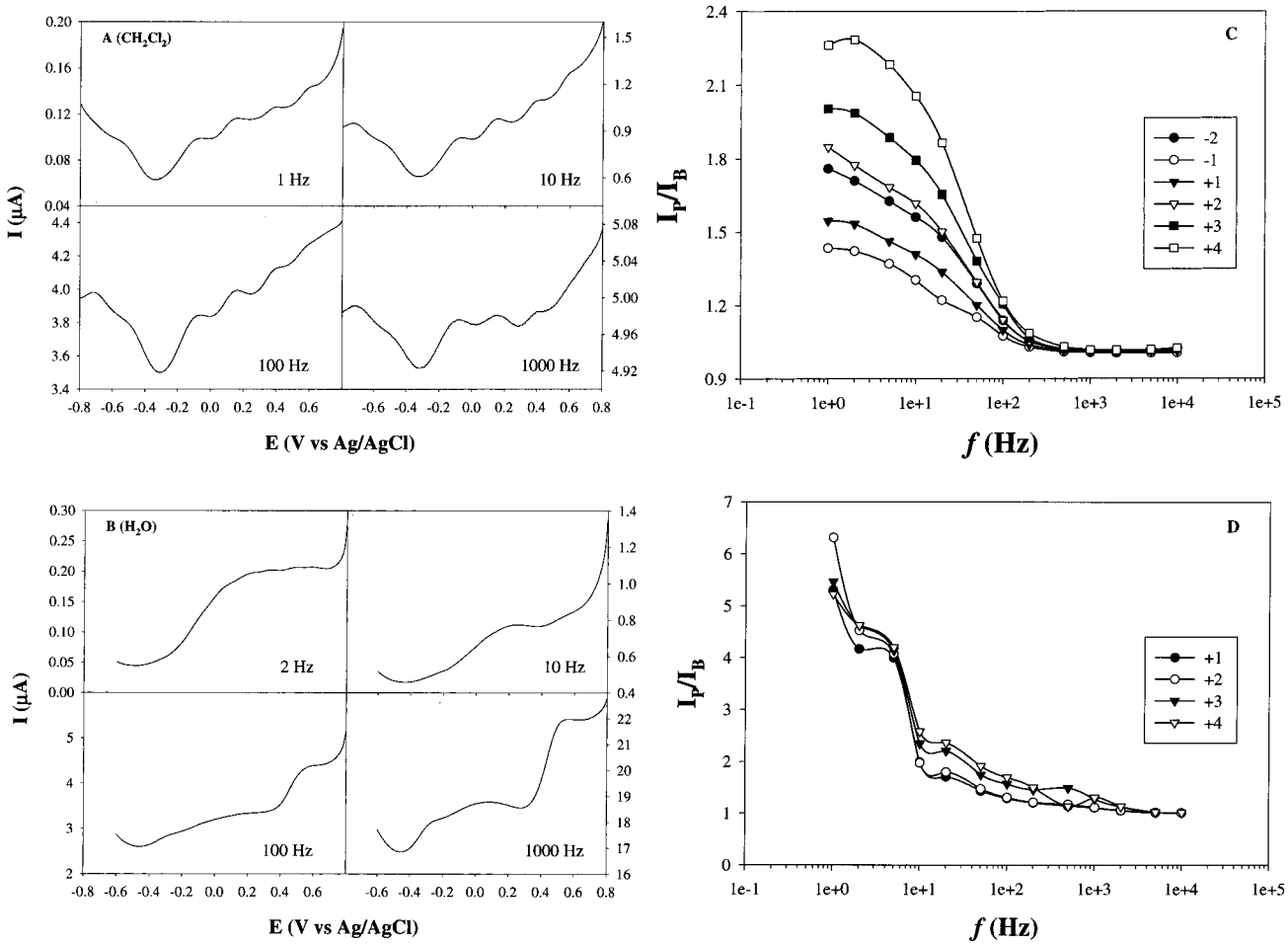

Figure 4. Ac voltammograms of a C6Au MPC monolayer in (A) CH_2Cl_2 containing 0.10 M TBAP; and (B) aqueous 0.10 M NH_4PF_6 solution. Electrode area ~1 mm^2. The dc potential ramp 10 mV/s, ac amplitude 10 mV, and the frequencies as shown. (C) and (D) show the variation of the ratios of the peak currents vs background current with ac frequency at varied MPC charge states in CH_2Cl_2 and aqueous solutions, respectively. Symbols are experimental data and lines are for guiding the eye only.

NH_4BF_4, TEAP, $TMABF_4$) < (NH_4NO_3, KNO_3) < ($TEANO_3$, $TMANO_3$). In other words, the effect of anion binding is decreasing in the order of PF_6^- > ClO_4^- ≈ BF_4^- > NO_3^-, which is in the same order of the ionic radii (and hydrophobicity), PF_6^- (0.255 nm) > ClO_4^- (0.226 nm) > BF_4^- (0.218 nm) > NO_3^- (0.165 nm).[14] Furthermore, the effects of cations on the onset potentials appear to be consistent with the ion hydrophobicity as well, where one can see that, in the presence of identical anions, the onset potential shifts anodically with increasing cation hydrophobicity, K^+ (0.151 nm) ≈ NH_4^+ (0.151 nm) < TEA^+ (0.265 nm) < TMA^+ (0.215 nm).[14]

These observations provide a mechanistic basis on which the potential regulation of MPC rectified quantized charging can be manipulated by electrolyte compositions. As mentioned above, the rectification of MPC quantized charging is more sensitive to electrolyte anions than to cations, in the context of the present experimental conditions, most probably due to the difference in solvation effect and interactions with charged nanoparticle molecules. However, at the moment, well-defined rectification can only be initiated at positive electrode potentials. To achieve rectification in the negative potential regime, one will have to extend the system to other bulky cationic species as well as to exploit structural manipulation of the MPC surface structures to enhance the MPC and electrolyte ion interactions that might lead to the chemical regulation of the interfacial double-layer capacitance. Further studies are currently underway.

Electron-Transfer Kinetics. The MPC quantized charging represents a novel electrochemical redox phenomenon, whose electron-transfer chemistry remains largely unexplored. Previously we used two electrochemical techniques to probe the kinetic aspects of these unique electron-transfer processes, one based on the Laviron method and the other based on ac voltammetry (or impedance spectroscopy).[7] Both methods yielded a rather consistent rate constant. We here describe some further studies using MPCs with varied protecting alkanethiolate chain lengths (and the corresponding alkanedithiol linkers), to examine the electron-transfer mechanism. Panels A and B of Figure 4 respectively show a series of ac voltammograms measured with a C6Au MPC monolayer in CH_2Cl_2 containing 0.10 M TBAP and in aqueous 0.10 M NH_4PF_6. One can see that, at low frequencies (e.g., 1 and 10 Hz), the quantized charging features of the surface MPC molecules are very visible, whereas at high frequencies (e.g., 200 and 1000 Hz), the discrete charge currents are only slightly larger than that of the background and become less well-defined. Panels C and D of Figure 4 show the corresponding plots of the variation of the ratio of the peak currents (I_P) versus background currents (I_B) with ac frequency. One can see that the overall behaviors are very similar to those observed with ω-ferrocenated alkanethiol monolayers on gold surfaces,[8,15] where at low frequencies, the

(14) (a) Jenkins, H. D. B.; Thakur, K. P. *J. Chem. Educ.* **1979**, *56*, 576. (b) Matsushita, N.; Kitagawa, H.; Mitani, T. *Synth. Met.* **1995**, *71*, 1933. (c) TMA^+ is more hydrophobic than TEA^+ despite its smaller ionic size, reflected in a lower solubility of its salts in water.

Table 3. Electron-Transfer Rate Constants (k_{Et}) of MPCs with Varied Protecting Ligands and Charge States (z) in Different Solution Media[a]

	z						
k_{et} (s^{-1})	−2	−1	+1	+2	+3	+4	average[b]
C4Au (CH_2Cl_2)	155	148	155	150	148	145	150.2 ± 4.1
C4Au (H_2O)			12	14	18	18	15.5 ± 3.0
C6Au (CH_2Cl_2)	63	48	50	60	68	55	57.3 ± 7.7
C6Au (H_2O)			7	7	7	7	7
C8Au (CH_2Cl_2)		3.1	3	3.1	3.2		3.1 ± 0.1

[a] In H_2O, 0.10 M NH_4PF_6 was used as the supporting electrolyte, while in CH_2Cl_2, 0.10 M TBAP was used instead. [b] Averaged over all charge states.

ratio I_P/I_B is much greater than 1 whereas at high frequencies, the ratio I_P/I_B approaches unity. This can be understood in terms of the relative amplitudes of the electron-transfer kinetics between the surface-confined MPC molecules and the electrode electrons versus the ac signal oscillation, and when the electron-transfer kinetics is not fast enough to keep up with the AC perturbation, the voltammetric responses start to level off. By fitting the curves with the Randles equivalent circuit (Scheme 1 inset), one can quantitatively estimate the corresponding electron-transfer rate constant for the MPC molecules,[15]

$$k_{et} = 1/2R_{CT}C_{SAM} \quad (2)$$

Similar observations are also found with other MPCs with different protecting ligands, with the results summarized in Table 3. It can be seen that the electron-transfer rate constants evaluated here generally fall within the range of $10-100\ s^{-1}$ and seem to vary only slightly with the charge states of the MPC molecules and increase with decreasing chain lengths of the MPC protecting monolayers. In addition, the kinetics appear to be somewhat faster in organic solutions than in aqueous media, which might be ascribed to the binding of electrolyte anions to the nanoparticles, rendering the energetic barrier greater for further oxidation of the MPC molecules. Another contributing factor might be related to the solvation of the alkanethiolate protecting monolayers in organic media, where the particles were squashed down so that the gold cores more closely approach the electrode surface.

For electron-tunneling through an organic barrier, the electron-transfer rate constant (k_{et}) has been found to decrease exponentially with the thickness of the barrier (d), $k_{et} \propto e^{-\beta d}$, with β being the coupling coefficient.[8] For straight alkyl spacers, the β values are typically found around $0.8-1.2\ Å^{-1}$.[8] Figure 5 shows the variation of the MPC electron-transfer rate constants in CH_2Cl_2 with the alkyl spacer length, where a relatively good linearity ($R^2 = 0.92$) can be seen. From the slope, one can estimate the β value to be $\sim 0.8\ Å^{-1}$. In the investigations of solid-state electronic conductivity of alkanethiolate-protected gold nanocluster molecules, Wuelfing et al. also obtained an electron-tunneling coefficient of $\beta = 0.8\ Å^{-1}$.[16a] This value is close to that found previously with two-dimensional self-assembled monolayers of alkanethiols with ω-functional groups (e.g., ferrocene).[8]

The above studies indicate that the electron-transfer kinetics of MPC molecules might not be as fast as one would think, which is a few orders of magnitude smaller than that of the ferrocene moiety tethered to a similar alkyl spacer on the electrode surface[8] or the electron self-exchange rate in nanoparticle multilayer thin films.[16b] Thus, one might argue that the rate constants measured above might actually reflect the ion-binding processes rather than the electron-transfer steps between MPCs and electrode. However, if this is the case, one would anticipate a rate constant (for a specific anion or cation) that is either invariant of the MPC structures or, more likely, (slightly) increasing with longer alkyl spacers due to increasing hydrophobicity of the particle protecting monolayers. This is contrary to the experimental observations shown above.

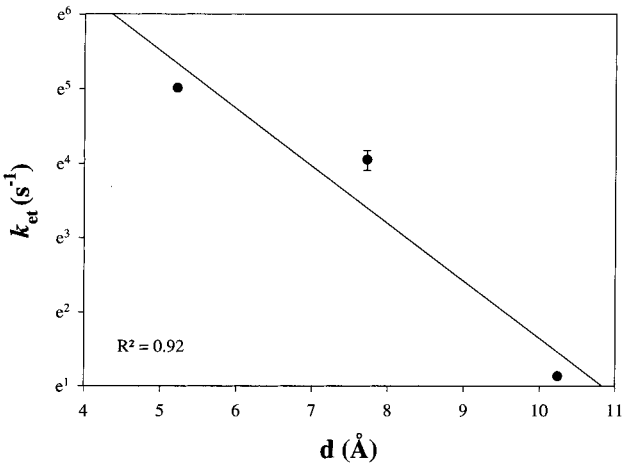

Figure 5. Variation of MPC electron-transfer rate constants with protecting ligand chain lengths in CH_2Cl_2 containing 0.10 M TBAP. Symbols are experimental data (Table 3) and line is the linear regression.

To provide further supporting evidence for the arguments presented above, we carried out additional studies to examine the MPC electron-transfer chemistry by employing an electroactive species as the probe molecule, such as dopamine. Figure 6A shows the cyclic voltammograms of 1 mM dopamine in 0.10 M KPF_6 at a naked gold electrode surface, where a pair of voltammetric waves can be found at +0.08 and +0.21 V (at 100 mV/s), respectively. These are ascribed to the 2-electron, 2-proton redox reactions of dopamine (DA) into dopamine-o-quinone (DOQ),[17]

$$DA \leftrightarrow DOQ + 2e^- + 2H^+ \quad (3)$$

Figure 6B depicts the variation of peak currents with the square roots of potential sweep rates where a good linearity is found, indicating diffusion-controlled reactions. However, the peak splitting ($\Delta E_p = 0.13$ V at 100 mV/s) is much greater than that expected for a reversible electron-transfer reaction (0.0285 V at $n = 2$, and 25 °C),[11] suggesting that the reaction is kinetically rather sluggish. Thus, one might suspect that if the MPC electron transfer is indeed very facile, they might be able to serve as electron-transfer mediators to facilitate the redox chemistry of dopamine. Or, if the MPC electron-transfer kinetics is not so fast, the redox processes of dopamine will be further impeded by the additional energetic barriers of MPC monolayers.

Figure 7A shows the cyclic voltammograms of the dopamine solution at a gold electrode with MPC monolayers with varied protecting monolayer ligands (the respective peak currents of dopamine redox reactions are again linearly proportional to the square root of potential sweep rates; not shown). One can see that the dopamine voltammetric currents are suppressed somewhat and the peak splitting becomes wider at MPC-modified electrodes than at the naked counterpart, indicating that the MPC

(15) Creager, S. E.; Wooster, T. T. *Anal. Chem.* **1998**, *70*, 4257.

(16) (a) Wuelfing, W. P.; Green, S. J.; Pietron, J. J.; Cliffel, D. E.; Murray, R. W. *J. Am. Chem. Soc.* **2000**, *122*, 11465. (b) Hicks, J. F.; Zamborini, F. P.; Osisek, A. J.; Murray, R. W. *J. Am. Chem. Soc.* **2001**, *123*, 7048.

(17) Tse, D. C. S.; McCreery, R. L.; Adams, R. N. *J. Med. Chem.* **1976**, *19*, 37.

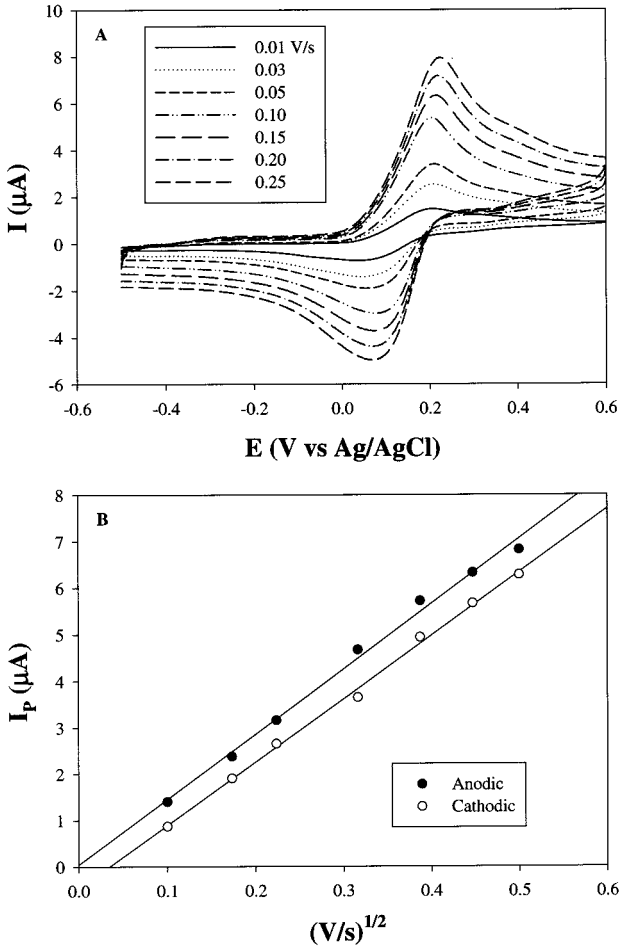

Figure 6. (A) CVs of 1 mM dopamine in 0.10 M KPF_6 at a naked gold electrode surface (area 0.167 mm^2) at varied sweep rates. (B) Variation of peak currents with the square roots of the sweep rates. Symbols are experimental data and lines are linear regressions.

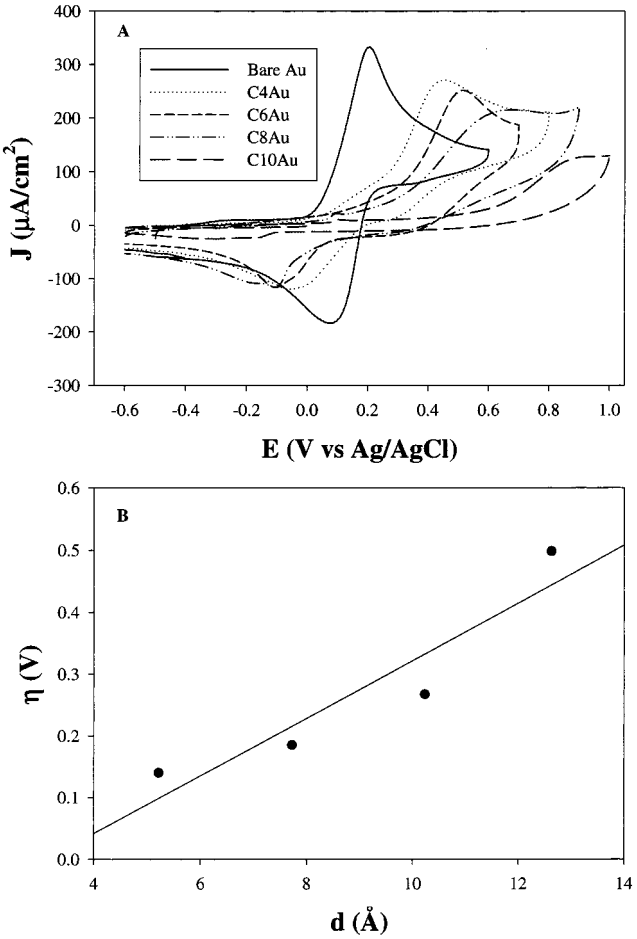

Figure 7. (A) CVs of 1 mM dopamine in 0.10 M KPF_6 at a gold electrode with MPC monolayers of varied protecting monolayers. Potential sweep rate 100 mV/s. (B) Variation of dopamine overpotentials with the MPC protecting ligand chain lengths. Symbols are experimental data and line is the linear regression.

monolayers in fact serve as a blocking layer against the dopamine electron transfer instead of being efficient electron-transfer mediators, as the overpotentials become even bigger with longer MPC protecting ligands. This implies that the electron-transfer kinetics of the MPC molecules cannot be very fast; in other words, the relatively sluggish electron-transfer kinetics of the MPC monolayers further slows down the relay of electron transfer for solution-phase dopamine to the electrode. Thus, the additional energetic barrier created by the MPC monolayers, Fη, has to be taken into account in the evaluation of the dopamine electron-transfer rate constants,[11]

$$k_f = k_{f,o}e^{-\alpha f\eta} \quad \text{and} \quad k_b = k_{b,o}e^{(1-\alpha)f\eta} \tag{4}$$

where η is the measured overpotential, subscripts f and b refer to forward and back reactions, respectively; subscript o denotes the rate constants at the naked electrode; $f = nF/RT$ (n, F, R, and T have their usual significance; and here $n = 2$); and α is the transfer coefficient. As a first-order approximation, it is assumed that the additional (effective) electron-transfer pathway involves electron tunneling through two alkanethiolate ligands and a metal core (Scheme 2), since it has been found that through-bond electron-transfer is much more favorable than the chain-to-chain path.[8b] That is, the rate constant should bear a similar exponential dependence on the particle organic layer thickness (d), $k \propto e^{-2\beta d}$. Thus, in combination with eq 4, one can obtain

Scheme 2. Schematic Chart of Electron-Tunneling through Surface-Confined Nanoparticle Layers

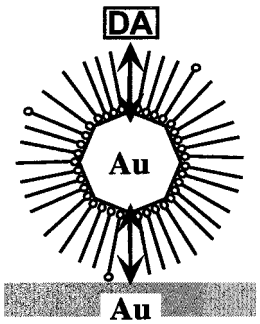

$$\eta \propto 2\beta d(RT/F) \tag{5}$$

by assuming $\alpha = 0.5$.[7] Figure 7B depicts the variation of overpotential with the alkanethiolate chain lengths (relative to the peak potential positions at the naked Au electrode).[18] One can see that the data points are not in good linearity as expected from eq 5, which might be ascribed to the oversimplification of modeling nanoparticle layers as a flat film with uniform thickness (equal to the particle diameter). However, for the sake

(18) Experimentally, it was found that the dopamine overpotentials increased with decreasing anion hydrophobicity, for instance, $\eta(NO_3^-) > \eta(PF_6^-)$, which might be related to the turn-on mechanism of the MPC rectified quantized charging as shown in Figure 2.

of a qualitative comparison, from the slope of the linear regression, one can obtain a β value of $\sim$0.9, which is somewhat greater than that calculated from the ac voltammetric measurements as shown above.

Concluding Remarks

Nanoparticle quantized charging can be rectified by hydrophobic electrolyte ions. It was found that the rectified charging features were more sensitive to anions than to cations in the experimental context of the current studies, with the onset potentials varied depending on the hydrophobicity and hence ion-binding strength of the ions. More importantly, a transition of the MPC charging responses was effected from those similar to conventional molecular diodes to those of quantized charging rectifiers by increasing anion hydrophobicity. Electron-transfer kinetics of these discrete charging processes did not appear to be very facile, with a rate constant typically within the range of 10−100 Hz and a coupling constant (β) of $\sim$0.8. In addition, using kinetically relatively sluggish dopamine as the probe molecules, we further examined the electron-transfer chemistry of MPC molecules, which provided additional supporting evidence for the MPC electron-transfer chemistry. The coupling constant evaluated from this method yielded a slightly larger value of 0.9. Further studies will focus on the structural manipulations of the electrolyte ions as well as the MPC molecules, which might provide a mechanistic basis to better control the ion-binding chemistry and hence the rectified MPC charging, as well as to explore their applications in the development of novel single-electron molecular diodes.

Acknowledgment. The authors are grateful to L. A. Truax and J. M. Sommers for their assistance in data collection during the early stage of the experiments. This work was supported by the National Science Foundation (CAREER Award), the Office of Naval Research, the ACS Petroleum Research Fund, the Illinois Department of Commerce and Community Affairs, and the SIU Materials Technology Center. S.C. is a Cottrell Scholar of the Research Corp.

JA011394C